A purified membrane protein from *Akkermansia muciniphila* or the pasteurized bacterium improves metabolism in obese and diabetic mice

Hubert Plovier[1], Amandine Everard[1*], Céline Druart[1*], Clara Depommier[1*], Matthias Van Hul[1], Lucie Geurts[1], Julien Chilloux[2], Noora Ottman[3#], Thibaut Duparc[4], Laeticia Lichtenstein[4], Antonis Myridakis[2], Nathalie M. Delzenne[1], Judith Klievink[5] Arnab Bhattacharjee[5], Kees C.H. van der Ark[3], Steven Aalvink[3], Laurent O. Martinez[4], Marc-Emmanuel Dumas[2], Dominique Maiter[6], Audrey Loumaye[6], Michel P. Hermans[6], Jean-Paul Thissen[6], Clara Belzer[3], Willem M. de Vos[3,5], Patrice D. Cani[1$]

[1]Université catholique de Louvain, Louvain Drug Research Institute, WELBIO (Walloon Excellence in Life sciences and BIOtechnology), Metabolism and Nutrition research group, B-1200 Brussels, Belgium,
[2] Division of Computational and Systems Medicine, Department of Surgery and Cancer, Imperial College London, Exhibition Road, South Kensington, London SW7 2AZ, United Kingdom,
[3] Laboratory of Microbiology, Wageningen University, Wageningen, The Netherlands.
[4] Institute of Metabolic and Cardiovascular Diseases, UMR1048, Inserm, Université de Toulouse, Toulouse, France,
[5]RPU Immunobiology, Department of Bacteriology & Immunology, University of Helsinki, Finland.
[6] Pole of Endocrinology, Diabetes and Nutrition; Institut de Recherche Expérimentale et Clinique IREC, Cliniques Universitaires Saint-Luc, Université catholique de Louvain, Brussels, Belgium

* These authors contributed equally to this work
[#] Current affiliation: Metapopulation Research Centre, University of Helsinki, Helsinki, Finland

[$] Correspondence to: Patrice.cani@uclouvain.be
Prof. Patrice D. Cani, Université catholique de Louvain, LDRI, Metabolism and Nutrition research group, Av. E. Mounier, 73 box B1.73.11, B-1200 Brussels, Belgium. Phone: +32 2 764 73 97

Obesity and type 2 diabetes are associated with low-grade inflammation and specific changes in gut microbiota composition[1-7]. We previously demonstrated that administration of *Akkermansia muciniphila* prevents the development of obesity and associated complications[8]. However, its mechanisms of action remain unclear, whilst the sensitivity of *A. muciniphila* to oxygen and the presence of animal-derived compounds in its growth medium currently limit the development of translational approaches for human medicine[9]. Here we addressed these issues by showing that *A. muciniphila* retains its efficacy when grown on a synthetic medium compatible with human administration. Unexpectedly, we discovered that pasteurization of *A. muciniphila* enhanced its capacity to reduce fat mass development, insulin resistance and dyslipidemia in mice. These improvements were notably associated with a modulation of the host urinary metabolomics profile and intestinal energy absorption. We demonstrated that Amuc_1100, a specific protein isolated from the outer membrane of *A. muciniphila*, interacts with Toll-Like Receptor 2, is stable at temperatures used for pasteurization, improves the gut barrier and partly recapitulates the beneficial effects of the bacterium. Finally, we showed that administration of live or pasteurized *A. muciniphila* grown on the synthetic medium is safe in humansThese findings provide support for the use of different preparations of *A. muciniphila* as therapeutic options to target human obesity and associated disorders.

Akkermansia muciniphila is one of the most abundant members of the human gut microbiota, representing between 1 and 5% of our intestinal microbes[10,11]. We and others recently observed that the abundance of *Akkermansia muciniphila* is decreased during obesity and diabetes[2,8] and is significantly associated with the improvement of cardiometabolic parameters in individuals with obesity undergoing caloric restriction[12]. Moreover, we found that daily administration of live *A. muciniphila* grown on a mucus-based medium can counteract the development of high-fat diet (HFD)-induced obesity and gut barrier dysfunction[8], an observation later confirmed by other groups[13,14]. However, the underlying mechanisms of these effects are still unclear. In addition, the current growth requirements of *A. muciniphila* and its oxygen sensitivity[9] render this bacterium unsuitable for human investigations and putative therapeutic opportunities.

Therefore, in HFD-fed mice, we compared the effects of daily administration of *A. muciniphila* grown either on a mucus-based medium (HFD Live Akk Mucus) or a synthetic medium where mucin was replaced by a combination of glucose, N-acetylglucosamine, soy peptone and threonine (HFD Live Akk Synthetic). This medium allowed us to culture *A. muciniphila* with the same efficiency as the mucus-based medium while being exempt of any compound incompatible with human administration. We observed that live *A. muciniphila* treatment tended to reduce HFD-induced body weight and fat mass gain (by about 40-50%) and to improve glucose intolerance and insulin resistance regardless of the growth medium used and independently of food intake (**Fig. 1a-g**).

We previously showed that autoclaving *A. muciniphila* abolished its beneficial effects[8]. However, recent investigations suggest that probiotics inactivated by pasteurization for 30 minutes at 70°C, a less extreme treatment limiting the denaturation of their cellular components, could partly or fully retain their beneficial effects[15,16]. Hence, we assessed the effects of *A. muciniphila* grown on a synthetic medium and inactivated by pasteurization (HFD Pasteurized Akk). Unexpectedly, in two separate sets of experiments, we found that pasteurized *A. muciniphila* exerted stronger effects than the live bacterium, as HFD-fed mice treated with pasteurized bacteria showed similar body weight and fat mass gain to mice fed with a control diet (ND), independently of food intake (**Fig. 1a-c** and **Supplemental Fig. 1a-c**). In both sets of experiments, we found that mice treated with pasteurized *A. muciniphila* displayed a much lower glucose intolerance and insulin concentration when compared to the HFD group, resulting in a lower insulin resistance (IR) index (**Fig. 1d-g** and **Supplemental Fig. 1d-g).** Treatment with pasteurized *A. muciniphila* also led to greater goblet cell density in the ileum when compared to ND-fed mice (**Fig. 1h**), suggesting a higher mucus production, while normalizing the mean adipocyte diameter (**Fig. 2a-b**) and significantly lowering plasma leptin when compared to HFD-fed mice (**Fig. 2c**). These effects were not observed in mice treated with live *A. muciniphila*. A similar trend could be observed for plasma resistin (**Supplemental Fig. 1h**), thereby suggesting improved insulin sensitivity, while plasma adiponectin remained unaffected in all conditions (**Supplemental Fig. 1i**). We found that mice treated with pasteurized *A. muciniphila* had a higher fecal caloric content when compared to all other groups (**Fig. 2d**), suggesting a lower energy absorption. This could contribute to the further reduction in body weight and fat mass gain observed in this group. Similar effects of *A. muciniphila* on energy absorption were previously

reported in mice undergoing cold exposure[17]. Altogether, these data suggest that pasteurization enhances the beneficial effects of *A. muciniphila* on HFD-induced metabolic syndrome. This could be due to increased accessibility of specific bacterial compounds involved in the positive effects of *A. muciniphila* on its host. Conversely, pasteurization of *A. muciniphila* could prevent the production of metabolites or factors mitigating its beneficial effects.

We next tested whether treatment with *A. muciniphila* could reduce the HFD-induced shift in the host urinary metabolome[18] HFD was the main factor influencing ^{1}H NMR-based untargeted metabolic profiles on the first O-PLS-DA score (Tpred1) while treatment with pasteurized *A. muciniphila* clustered separately from all other groups regarding the second score (Tpred2) (**Fig. 2e-g**). This resulted in a normalization of the HFD-induced shift of 37% with the pasteurized bacterium, and 17% with the live bacterium (**Fig. 2f**).

By comparing the metabolic profiles of the different groups, we found that the shift induced by pasteurized *A. muciniphila* was mainly associated with trimethylamine (TMA) and trimethylamine-*N*-oxide (TMAO) according to the OPLS-DA model coefficients (**Supplemental Fig. 2**). While HFD feeding severely lowered the abundance of TMA compared to ND-fed mice, treatment with pasteurized *A. muciniphila* significantly offset this reduction (**Fig. 2h**). A similar trend was observed for urinary TMAO (**Fig. 2i**). This relative increase in TMA abundance was not observed in mice treated with live *A. muciniphila*. Treatment with pasteurized *A. muciniphila* also modulated hepatic expression of *Fmo3*, encoding the Flavin monooxygenase 3 that converts TMA to TMAO, a metabolite associated with atherosclerosis[19,20]. While exposure to a HFD led to a two-fold higher *Fmo3* expression when compared to ND-fed mice, treatment with pasteurized *A. muciniphila* reversed this effect (**Fig. 2j**). Of note, knockdown of *Fmo3* by the use of specific antisense oligonucleotides can increase serum concentration of TMA[20] and protects mice against the development of atherosclerosis and insulin resistance[21]. Moreover, recent findings suggest that oral administration of live *A. muciniphila* can impede atherosclerosis development in *Apoe*$^{-/-}$ mice[22]. In our study however, the effects observed on urinary TMA and *Fmo3* expression were not associated with a modification of plasma TMA and TMAO, as all HFD-fed group displayed similar concentrations for both metabolites (**Fig. 2k**,**l**). This suggests that the observed decrease in *Fmo3* expression is not sufficient to inhibit the conversion of TMA in TMAO, and that metabolic effects of pasteurized *A. muciniphila* are not related to these metabolites.

Toll-like receptors (TLRs) regulate bacterial recognition, intestinal homeostasis and can also shape the host metabolism[23-25]. To identify how *A. muciniphila* interacts with its host, we performed *in vitro* experiments to evaluate its TLR signaling potential. Previous results suggested that *A. muciniphila* lipopolysaccharide (LPS) differs structurally from that of *E. coli* and is not a powerful TLR4 agonist[26]. Here, we observed that *A. muciniphila* specifically activated cells expressing TLR2 (**Fig. 3a**), but not cells expressing TLR5, TLR9 or the NOD2 receptor (**Fig. 3b-d**).

Genomic and proteomic analyses of *A. muciniphila* identified proteins encoded by a specific Type IV pili gene cluster in fractions enriched for outer membrane proteins[27]. Among these, Amuc_1100 was one of the most abundant. Additionally, its presence on a gene cluster related to pilus formation suggests that it could be involved in the crosstalk with the host. To test this hypothesis, we showed that a His-tagged Amuc_1100 produced in *E. coli* (hereafter called Amuc_1100*) could signal to TLR2-expressing cells in a similar manner to *A. muciniphila* (**Fig. 3a**). Furthermore, Amuc_1100* appeared relatively thermostable as differential light scattering analysis indicated its melting temperature was 70°C (**Fig. 3e**), which is the temperature applied for pasteurization. Therefore, Amuc_1100 could still be active in pasteurized bacteria and contribute to the observed signaling.

Consequently, we compared the effects of the live and pasteurized bacterium to those of Amuc_1100* in HFD-fed mice. Similarly to what was observed with the pasteurized bacterium, treatment with Amuc_1100* induced a lower body weight and fat mass gain when compared to untreated HFD-fed mice, independently of food intake (**Fig. 3f-h**). It also tended to correct HFD-induced higher adipocyte diameter (**Supplemental Fig. 3a**,**b**). Treatment with *A. muciniphila* or Amuc_1100* corrected HFD-induced hypercholesterolemia, with significantly lower plasma HDL-cholesterol concentrations and a similar trend for LDL-cholesterol (**Fig. 3i**). Mice treated with pasteurized *A. muciniphila* displayed significantly lower plasma triglycerides concentrations when compared to either untreated mice or HFD-fed mice treated with live *A. muciniphila*, again suggesting an increased potency of the bacterium after pasteurization (**Fig. 3j**). No differences were observed in the distribution of triglycerides and cholesterol in lipoproteins (**Supplemental Fig. 3c-d**). Amuc_1100* also improved glucose tolerance with the same potency as the live and pasteurized bacterium (**Fig. 3k**,**l**). To further investigate the effects of *A. muciniphila* on insulin sensitivity, we analyzed insulin-induced phosphorylation of the insulin receptor (IR) and its

downstream mediator Akt at the threonine (Akt^{thr}) and serine (Akt^{ser}) sites[28] in the liver (**Fig. 3m**,**n**). As previously described, untreated HFD-fed mice displayed lower phosphorylation of all analyzed proteins when compared to ND-fed mice[29], reaching significance for Akt^{thr} (**Fig. 3n**). Treatment with *A. muciniphila* or Amuc_1100* counteracted these effects, with significantly higher levels of p-IR and p-Akt^{thr} in mice treated with Amuc_1100* (**Fig. 3m-n**) and significantly higher levels of p-Akt^{ser} in mice treated with the live bacterium (**Fig. 3n**) when compared to untreated HFD-fed mice.

Previous reports show that beneficial effects of *A. muciniphila* are associated to improvements of the gut barrier function[8,13,22,26] leading to a correction of metabolic endotoxemia (*i.e.* increased portal LPS concentration) in obese and diabetic mice. We therefore assessed the effects of pasteurized *A. muciniphila* and Amuc_1100* on endotoxemia and genes associated with the intestinal barrier. While HFD-fed mice displayed higher portal LPS concentration than ND-fed mice, treatment with *Akkermansia* –either live or pasteurized– or Amuc_1100* completely restored LPS concentration to that observed in the ND group (**Fig. 4a**). Among the assessed markers of the gut barrier, we found that expression of *Cnr1*, coding for the cannabinoid receptor 1 (CB_1), was specifically lower in the jejunum of mice treated with Amuc_1100* (**Fig. 4b**). Interestingly, activation of CB_1 was shown to increase intestinal permeability *in vitro*, whereas blocking CB_1 reduces gut permeability both *in vitro* and *in vivo*[30]. Consistently with these findings, genes encoding tight-junction proteins involved in the regulation of intestinal permeability were also affected. In the jejunum, expression of *Cldn3* (encoding Claudin3) was higher in mice treated with Amuc_1100* when compared to untreated HFD-fed mice (**Fig. 4b**) while *Ocln* (encoding Occludin) was higher in all treated groups when compared to ND-fed mice, as well as when comparing untreated HFD-fed mice with mice receiving Amuc_1100* (**Fig. 4b**). In the ileum, a trend for lower *Cnr1* expression was observed following treatment with *A. muciniphila* (**Fig. 4c**). *Cldn3* expression was greater in all treated groups when compared to untreated ND- and HFD-fed mice, while *Ocln* was unaffected (**Fig. 4c**). These effects could notably be explained by the ability of *A. muciniphila* to activate TLR2 *via* Amuc_1100, as this receptor can regulate various tight-junction proteins including Occludin and Claudin 3[31,32]. In the colon, untreated HFD-fed mice had a higher *Ocln* expression as compared to the other groups, whereas *Cnr1* tended to be higher in all HFD-fed groups and *Cldn3* was not modified (**Supplemental Fig. 4a**).

We next assessed markers of the synthesis (*Napepld*) and the degradation (*Naaa*) of different endocannabinoids and bioactive lipids from the *N*-acylethanolamine (NAEs) family[33]. *Napepld* expression was lower specifically in the jejunum following treatment with pasteurized *A. muciniphila* when compared to ND-fed mice or mice treated with Amuc_1100* (**Supplemental Fig. 4b**). *Naaa* however was not modified by any treatment in all intestinal segments (**Supplemental Fig. 4b-d**). Therefore, this set of data suggests that Amuc_1100* and pasteurized *A. muciniphila* exhibited distinct mechanisms of action on the endocannabinoid system.

Antimicrobial peptides are also contributing to the gut barrier function by shaping the gut microbiota[34]. We found that mice treated with pasteurized *A. muciniphila* had significantly higher *Lyz1* expression in both the jejunum and ileum when compared to ND-fed mice, while Amuc_1100* did not significantly affect this parameter (**Fig. 4d**,**e**). We observed a significantly lower *DefA* expression in the jejunum of mice treated with pasteurized *A. muciniphila* and Amuc_1100* as compared to ND-fed mice (**Fig. 4d**). In the ileum, mice treated with Amuc_1100* had significantly lower *DefA* expression as compared to mice treated with either live or pasteurized *A. muciniphila* (**Fig. 4e**). This again suggests different mechanisms of action of Amuc_1100* and pasteurized *A. muciniphila,* here on antimicrobial peptides. However, treatment with *A. muciniphila* or Amuc_1100* did not change the HFD-mediated lower *Reg3g and Pla2g2* expression (**Fig. 4d**,**e** and **Supplemental Fig. 4e**). Altogether, these results suggest that Amuc_1100* and pasteurized *A. muciniphila* act on different targets to reinforce the intestinal barrier in the jejunum and ileum, which could explain the correction of HFD-induced metabolic endotoxemia in treated mice.

Finally, we evaluated the safety and tolerability of *A. muciniphila* in individuals with excess body weight by treating them with different doses of live *A. muciniphila* (Akk Synthetic - 10^{10} and Akk Synthetic - 10^{9}) or pasteurized *A. muciniphila* (Akk Pasteurized - 10^{10}) as part of an ongoing clinical study testing the efficacy of this bacterium on metabolic parameters associated with obesity and the metabolic syndrome. Subjects are currently being recruited and analyzed, and complete results will be reported once the study is complete (end of 2017). Anthropomorphic characteristics of the subjects at the beginning of treatment are reported in Supplemental **Table 1**. We analyzed several clinical parameters measured in probiotics safety assessments[35-37] before and after two weeks of treatment. No significant changes on markers related to inflammation and

hematology, kidney, liver and muscle function were observed with any formulation of *A. muciniphila* (**Supplemental Fig. 5** and Supplemental **Table 2**). Moreover, the frequency of recorded adverse effects was similar in all groups (Supplemental **Table 3**). Borborygmi were reported by some subjects treated with live *A. muciniphila*, but the difference with other groups was not significant. While the number of subjects is limited, these first human data suggest that both live and pasteurized *A. muciniphila* are well tolerated in subjects with excess body weight and appear safe for oral administration in the context of obesity.

A. muciniphila is a promising target in the management of obesity and related disorders. Several studies have shown positive associations between *A. muciniphila* and the host metabolic health. Moreover, various dietary interventions targeting obesity and glucose intolerance increase *A. muciniphila* abundance[8,34,38] as does the glucose-lowering drug metformin[3,13]. To our knowledge, *A. muciniphila* is currently unique in the field of next-generation probiotic research as it resides in the mucus layer, a niche in close vicinity of host cells, and because it displays beneficial effects on several pathologies. Direct administration has proven protective not only against obesity but also against type 2 diabetes, gut barrier disturbances as well as atherosclerosis in various studies[8,13,14,22]. Moreover, metagenomics data suggest that *A. muciniphila* abundance could also be inversely associated with type 1 diabetes and inflammatory bowel disorders[39,40]. However, translational evaluation of *A. muciniphila* for human therapeutics is hampered by the requirement for animal-derived compounds in the growth medium of the bacterium. To circumvent this issue, we tested the effects of *A. muciniphila* grown on a synthetic medium compatible with human administration. We show in mice that effects on obesity and glucose metabolism are generally conserved when compared to the bacterium grown on a mucus-based medium.

Another hurdle to the use of live *A. muciniphila* in human subjects is its high sensitivity to oxygen. Here, we show that non-replicative, pasteurized *A. muciniphila* had stronger effects on body weight gain, fat mass gain and glucose intolerance in HFD-fed mice. These effects are associated with specific modulations of the host urinary metabolome, decreased intestinal energy absorption, normalization of plasma LPS concentration and decreased triglyceridemia. Moreover, we show that the outer membrane protein Amuc_1100* is involved in the *A. muciniphila*-to-host interaction through TLR2 signaling, and that it partially recapitulates the effects of *A. muciniphila* against obesity, insulin resistance and gut barrier alteration. How pasteurization enhances the

effects of *A. muciniphila* remains to be elucidated. The fact that Amuc_1100* is still stable at 70°C suggests it could still be signaling in pasteurized cells and that pasteurization enhances the effects of *A. muciniphila* by increasing accessibility of this protein to the host. Whether this improvement of beneficial effects through pasteurization is specific to *A. muciniphila* or could be extended to other bacteria also needs to be tested. Regardless, pasteurization could represent an innovative way to use anaerobic strains as a therapeutic tool. Moreover, identification and isolation of specific bacterial products recapitulating all or part of the effects of the live organism could prove useful in the treatment of conditions such as inflammatory bowel diseases, where direct administration of live probiotics would be challenging.

Finally, preliminary human data suggest that treatment with either live or pasteurized *A. muciniphila* grown on the synthetic medium is safe in individuals with excess body weight, as no changes in relevant safety clinical parameters or reported adverse events were observed after two weeks of treatment. These results pave the way for future human studies investigating *A. muciniphila* as a therapeutic tool in the management of the metabolic syndrome.

Data availability

The data that support the findings of this study are available from the corresponding author upon reasonable request.

Acknowledgements

We wish to thank A. Barrois, H. Danthinne, M. De Barsy, R-M. Goebbels and T. Pringels for excellent technical assistance. We wish to thank S. Matamoros for helpful discussion and help during tissue sampling. We also wish to thank the individuals who participated in this study. HP is a research fellow at FRS-FNRS (Fonds de la Recherche Scientifique), Belgium. PDC is a research associate at FRS-FNRS (Fonds de la Recherche Scientifique), Belgium. AE is a postdoctoral researcher at FRS-FNRS, Belgium. CD researcher position is supported by a FIRST Spin-Off grant from the Walloon Region (convention 1410053). Research in the Wageningen and Helsinki labs of WMdV was partially supported by ERC Advanced Grant 250172 (Microbes Inside), the SIAM Gravity Grant 024.002.002 and Spinoza Award of the Netherlands Organization for Scientific Research, and Grants 137389, 141140 and 1272870 of the Academy

of Finland. PDC is the recipient of grants from FNRS (convention J.0084.15, convention 3.4579.11), PDR (Projet de Recherche, convention: T.0138.14) and ARC (Action de Recherche Concertée - Communauté française de Belgique convention: 12/17-047). This work was supported by the FRFS-WELBIO under grant: WELBIO-CR-2012S-02R. This work is supported in part by the Funds Baillet Latour (Grant for Medical Research 2015), a FIRST Spin-Off grant (FSO) from the Walloon Region, Belgium (convention 1410053) and FP7 METACARDIS (HEALTH-F4-2012-305312). PDC is a recipient of POC ERC grant 2016 (European Research Council, Microbes4U_713547) and ERC Starting Grant 2013 (Starting grant 336452-ENIGMO).

Author contributions

PDC and WMdV conceived the project. PDC supervised the preclinical and clinical part and WMdV the microbial culturing and expression part. PDC and HP designed the mouse experiments, performed experiments and interpreted all the results, generated figures and tables and wrote the manuscript; AE, CDr, MVH, LG, CDe performed experiments. JC, AM and MED performed ^{1}H-NMR and UPLC-MS metabolomic analyses. TD, LL, LOM analyzed plasma lipoprotein profiles. CB, KCHvdA, HP, CD and SA performed the culturing and pasteurization of A. muciniphila. JK produced and purified Amuc_1100*, which was structurally analyzed by AB. In vitro analysis of A. muciniphila and Amuc_1100* signaling was carried out by NO and CB. JPT, MH, AL, DM, AE, CDr, CDe, WMdV and PDC designed the clinical study. JM, AL, MH, JPT screened the subjects and contributed to follow-up. AE, CDr, CDe, PDC, followed subjects during the study. All authors discussed results and approved the manuscript.

Competing financial interests

HP, AE, CDr, PDC, CB and WMdV are inventors on patent applications dealing with the use of *A.muciniphila* and its components in the treatment of obesity and related disorders.

References

1. Qin, J., *et al.* A metagenome-wide association study of gut microbiota in type 2 diabetes. *Nature* **490**, 55-60 (2012).
2. Le Chatelier, E., *et al.* Richness of human gut microbiome correlates with metabolic markers. *Nature* **500**, 541-546 (2013).
3. Forslund, K., *et al.* Disentangling type 2 diabetes and metformin treatment signatures in the human gut microbiota. *Nature* **528**, 262-266 (2015).
4. Ridaura, V.K., *et al.* Gut microbiota from twins discordant for obesity modulate metabolism in mice. *Science* **341**, 1241214 (2013).
5. Turnbaugh, P.J., *et al.* An obesity-associated gut microbiome with increased capacity for energy harvest. *Nature* **444**, 1027-1031 (2006).
6. Cani, P.D., *et al.* Metabolic endotoxemia initiates obesity and insulin resistance. *Diabetes* **56**, 1761-1772 (2007).
7. Everard, A., *et al.* Intestinal epithelial MyD88 is a sensor switching host metabolism towards obesity according to nutritional status. *Nature communications* **5**, 5648 (2014).
8. Everard, A., *et al.* Cross-talk between Akkermansia muciniphila and intestinal epithelium controls diet-induced obesity. *Proc Natl Acad Sci U S A* **110**, 9066-9071 (2013).
9. Derrien, M., Vaughan, E.E., Plugge, C.M. & de Vos, W.M. Akkermansia muciniphila gen. nov., sp. nov., a human intestinal mucin-degrading bacterium. *International journal of systematic and evolutionary microbiology* **54**, 1469-1476 (2004).
10. Collado, M.C., Derrien, M., Isolauri, E., de Vos, W.M. & Salminen, S. Intestinal integrity and Akkermansia muciniphila, a mucin-degrading member of the intestinal microbiota present in infants, adults, and the elderly. *Appl Environ Microbiol* **73**, 7767-7770 (2007).
11. Derrien, M., Collado, M.C., Ben-Amor, K., Salminen, S. & de Vos, W.M. The Mucin degrader Akkermansia muciniphila is an abundant resident of the human intestinal tract. *Appl Environ Microbiol* **74**, 1646-1648 (2008).
12. Dao, M.C., *et al.* Akkermansia muciniphila and improved metabolic health during a dietary intervention in obesity: relationship with gut microbiome richness and ecology. *Gut* **65**, 426-436 (2016).
13. Shin, N.R., *et al.* An increase in the Akkermansia spp. population induced by metformin treatment improves glucose homeostasis in diet-induced obese mice. *Gut* **63**, 727-735 (2014).
14. Org, E., *et al.* Genetic and environmental control of host-gut microbiota interactions. *Genome research* **25**, 1558-1569 (2015).
15. Peng, G.C. & Hsu, C.H. The efficacy and safety of heat-killed Lactobacillus paracasei for treatment of perennial allergic rhinitis induced by house-dust mite. *Pediatr Allergy Immunol* **16**, 433-438 (2005).
16. Sakai, T., *et al.* Lactobacillus plantarum OLL2712 regulates glucose metabolism in C57BL/6 mice fed a high-fat diet. *Journal of nutritional science and vitaminology* **59**, 144-147 (2013).
17. Chevalier, C., *et al.* Gut Microbiota Orchestrates Energy Homeostasis during Cold. *Cell* **163**, 1360-1374 (2015).
18. Dumas, M.E., *et al.* Metabolic profiling reveals a contribution of gut microbiota to fatty liver phenotype in insulin-resistant mice. *Proc Natl Acad Sci U S A* **103**, 12511-12516 (2006).
19. Koeth, R.A., *et al.* Intestinal microbiota metabolism of L-carnitine, a nutrient in red meat, promotes atherosclerosis. *Nature medicine* **19**, 576-585 (2013).
20. Bennett, B.J., *et al.* Trimethylamine-N-oxide, a metabolite associated with atherosclerosis, exhibits complex genetic and dietary regulation. *Cell metabolism* **17**, 49-60 (2013).
21. Miao, J., *et al.* Flavin-containing monooxygenase 3 as a potential player in diabetes-associated atherosclerosis. *Nature communications* **6**, 6498 (2015).
22. Li, J., Lin, S., Vanhoutte, P.M., Woo, C.W. & Xu, A. Akkermansia Muciniphila Protects Against Atherosclerosis by Preventing Metabolic Endotoxemia-Induced Inflammation in Apoe-/- Mice. *Circulation* (2016).
23. Shi, H., *et al.* TLR4 links innate immunity and fatty acid-induced insulin resistance. *The Journal of clinical investigation* **116**, 3015-3025 (2006).

24. Abreu, M.T. Toll-like receptor signalling in the intestinal epithelium: how bacterial recognition shapes intestinal function. *Nature reviews. Immunology* **10**, 131-144 (2010).
25. Vijay-Kumar, M.*, et al.* Metabolic syndrome and altered gut microbiota in mice lacking Toll-like receptor 5. *Science* **328**, 228-231 (2010).
26. Reunanen, J.*, et al.* Akkermansia muciniphila adheres to enterocytes and strengthens the integrity of epithelial cell layer. *Applied and environmental microbiology* (2015).
27. Ottman, N.*, et al.* Characterization of Outer Membrane Proteome of Akkermansia muciniphila Reveals Sets of Novel Proteins Exposed to the Human Intestine. *Frontiers in microbiology* **7**, 1157 (2016).
28. Taniguchi, C.M., Emanuelli, B. & Kahn, C.R. Critical nodes in signalling pathways: insights into insulin action. *Nature reviews. Molecular cell biology* **7**, 85-96 (2006).
29. Liu, Z.*, et al.* High-fat diet induces hepatic insulin resistance and impairment of synaptic plasticity. *PloS one* **10**, e0128274 (2015).
30. Muccioli, G.G.*, et al.* The endocannabinoid system links gut microbiota to adipogenesis. *Molecular systems biology* **6**, 392 (2010).
31. Cario, E., Gerken, G. & Podolsky, D.K. Toll-like receptor 2 controls mucosal inflammation by regulating epithelial barrier function. *Gastroenterology* **132**, 1359-1374 (2007).
32. Gu, M.J.*, et al.* Barrier protection via Toll-like receptor 2 signaling in porcine intestinal epithelial cells damaged by deoxynivalnol. *Vet Res* **47**, 25 (2016).
33. Cani, P.D.*, et al.* Endocannabinoids - at the crossroads between the gut microbiota and host metabolism. *Nature reviews. Endocrinology* **12**, 133-143 (2016).
34. Everard, A.*, et al.* Microbiome of prebiotic-treated mice reveals novel targets involved in host response during obesity. *The ISME journal* (2014).
35. Jones, M.L., Martoni, C.J., Di Pietro, E., Simon, R.R. & Prakash, S. Evaluation of clinical safety and tolerance of a Lactobacillus reuteri NCIMB 30242 supplement capsule: a randomized control trial. *Regulatory toxicology and pharmacology : RTP* **63**, 313-320 (2012).
36. Burton, J.P.*, et al.* Evaluation of safety and human tolerance of the oral probiotic Streptococcus salivarius K12: a randomized, placebo-controlled, double-blind study. *Food Chem Toxicol* **49**, 2356-2364 (2011).
37. Wind, R.D., Tolboom, H., Klare, I., Huys, G. & Knol, J. Tolerance and safety of the potentially probiotic strain Lactobacillus rhamnosus PRSF-L477: a randomised, double-blind placebo-controlled trial in healthy volunteers. *The British journal of nutrition* **104**, 1806-1816 (2010).
38. Everard, A.*, et al.* Responses of gut microbiota and glucose and lipid metabolism to prebiotics in genetic obese and diet-induced leptin-resistant mice. *Diabetes* **60**, 2775-2786 (2011).
39. Brown, C.T.*, et al.* Gut microbiome metagenomics analysis suggests a functional model for the development of autoimmunity for type 1 diabetes. *PloS one* **6**, e25792 (2011).
40. Png, C.W.*, et al.* Mucolytic bacteria with increased prevalence in IBD mucosa augment in vitro utilization of mucin by other bacteria. *The American journal of gastroenterology* **105**, 2420-2428 (2010).

Figure legends

Figure 1 Pasteurization enhances *A. muciniphila*-mediated effects on high-fat diet-induced obesity. (**a**,**b**) Body weight gain (**a**) and fat mass gain (**b**) in grams after 4 weeks of treatment. (**c**) Daily food intake per mouse in grams. (**d**) Plasma glucose (mg dl^{-1}) profile and (**e**) the mean area under the curve (AUC) measured during an oral tolerance test (OGTT) (mg.dl^{-1}.min^{-1}). (**f**) Plasma insulin (µg l^{-1}) measured at T-30 min and T+15 min during the OGTT. (**g**) Insulin resistance index. (**h**) Ileum goblet cell density. Data are presented as the mean ± s.e.m. Number of mice per group for **a**,**b**: ND: 9, HFD: 8, HFD Live Akk Mucus: 9, HFD Live Akk Synthetic: 10, HFD Pasteurized Akk: 8. For **c**, 5 measurements were obtained for each group. Number of mice per group for **d-g**: ND: 9, HFD: 8, HFD Live Akk Mucus: 9, HFD Live Akk Synthetic: 10, HFD Pasteurized Akk: 7. Number of mice per group for **h**: ND: 7, HFD: 8, HFD Live Akk Mucus: 8, HFD Live Akk Synthetic: 8, HFD Pasteurized Akk: 7. Data were analyzed using one-way ANOVA followed by Tukey post-hoc test for **a**, **b**, **c**, **e, g** and **h,** and according to two-way ANOVA followed by Bonferonni post-hoc test for **d** and **f**. * $P < 0.05$; ** $P < 0.01$; *** $P < 0.001$.

Figure 2 Pasteurized *A. muciniphila* modulates adipose tissue physiology, intestinal energy absorption and urinary metabolome. (**a**) Representative hematoxylin and eosin-stained pictures of subcutaneous adipose tissue (SAT) deposits (n = 5 images per mouse). Scale bar, 100 µm. (**b**) Mean adipocyte diameter (µm) in the SAT. (**c**) Plasma leptin (ng ml^{-1}). (**d**) Fecal energetic content (kcal g $feces^{-1}$). (**e**) Orthogonal Partial Least Squares discriminant analysis (OPLS-DA) predictive score plot for urine metabolic profiles representing predictive component 1 (Tpred1) vs Tpred2. (**f**) Projection of all treatment groups on the first predictive score of the OPLS-DA model. (**g**) Empirical assessment of the significance of O-PLS goodness-of-fit parameters. (**h-i**) Relative abundance of urinary (**h**) trimethylamine (TMA) and (**i**) trimethylamine-N-oxide (TMAO). (**j**) mRNA expression of hepatic Flavin-containing monooxygenase 3. (**k**) Plasma TMA (µM). (**l**) Plasma TMAO (µM). Data are presented as the mean ± s.e.m. Number of mice per group for **a-c** and **j-l**: ND: 10, HFD: 8, HFD LiveAkk Synthetic: 10, HFD Pasteurized Akk: 9. For **d**, 5 measurements were obtained for each group. Number of mice per group for **e-i**: ND: 5, HFD: 7, HFD Live Akk Synthetic: 5, HFD Pasteurized Akk: 5. Data were analyzed using one-

way ANOVA followed by a Tukey post-hoc test for **b-d**, and **h-k.** * $P < 0.05$; ** $P < 0.01$; *** $P < 0.001$.

Figure 3 *A. muciniphila* protein Amuc_1100* recapitulates the effects of the pasteurized bacterium on diet-induced obesity. (**a-d**) Stimulation of human HEK-Blue cells expressing (**a**) human Toll-Like Receptor (TLR) 2, (**b**) TLR5, (**c**) TLR9 and (**d**) human NOD2 receptor. (**e**) Dynamic light scattering analysis of Amuc_1100* folding state according to the temperature. (**f**,**g**) Total body weight gain (**f**) and total fat mass gain (**g**) in grams after 5 weeks of treatment. (**h**) Daily food intake per mouse (g). (**i**) Plasma VLDL, LDL and HDL cholesterol (mg dl^{-1}). (**j**) Plasma triglycerides (mg dl^{-1}). (**k**) Plasma glucose (mg dl^{-1}) profile and (**e**) the mean area under the curve (AUC) measured during an oral tolerance test ($mg.dl^{-1}.min^{-1}$). (**m**) Representative western-blot of 4 total western-blots for hepatic p-IRβ and β-actin with or without insulin stimulation. Ratio of the vehicle- and insulin-stimulated p-IRβ on the loading control measured by densitometry. (**n**) Representative western-blot of 4 total western-blots for hepatic p-Akt^{thr308}, p-Akt^{ser473} and β-actin with or without insulin stimulation. Ratio of the vehicle- and insulin-stimulated p-Akt^{thr308} and p-Akt^{ser473} on the loading control measured by densitometry. Full-length blots are shown in **Supplemental Fig. 6** and **Supplemental Fig. 7**. Data are presented as the mean ± s.e.m. Data in panels **a, c** and **d** represent 3 independent experiments, except for low concentrations of Amuc_1100* (0.05 and 0.5 μg/ml), where 2 independent experiments were performed. Data in panel **b** represent 2 independent experiments. Number of mice per group for **f**, **g**, **i**, **k** and **l**: ND: 9, HFD: 8, HFD Live Akk Synthetic: 8, HFD Pasteurized Akk: 10, HFD Amuc_1100*: 10. For **h**, 5 measurements were obtained for each group. Number of mice per group for **j**: ND: 9, HFD: 8, HFD Live Akk Synthetic: 8, HFD Pasteurized Akk: 10, HFD Amuc_1100*: 9. Number of mice per group for **m-n**: ND: 8, HFD: 9, HFD Live Akk Synthetic: 9, HFD Pasteurized Akk: 9, HFD Amuc_1100*: 9. Data were analyzed using one-way ANOVA followed by Dunnett post-hoc test versus DMEM condition for **a**, **c** and **d**, using Kruskal-Wallis followed by Dunns post-hoc test versus DMEM condition for **b**, according to one-way ANOVA followed by Tukey post-hoc test for **f**, **g**, **h**, **j**, and **l**, and according to two-way ANOVA followed by Bonferonni post-hoc test for **i**, **k**, **m** and **n**.* $P < 0.05$; ** $P < 0.01$; *** $P < 0.001$.

Figure 4 Effects of *A. muciniphila* or Amuc_1100* on the intestinal barrier function. (**a**) Portal plasma LPS (EU/ml). (**b**) Expression of *Cnr1*, *Cldn3* and *Ocln* in the jejunum. (**c**) Expression of *Cnr1*, *Cldn3* and *Ocln* in the ileum. (**d**) Expression of *Lyz1, DefA*, *Reg3g* and *Pla2g2* in the jejunum. (**e**) Expression of *Lyz1, DefA*, *Reg3g* and *Pla2g2* in the ileum. Data are presented as the mean $\pm$ s.e.m. Number of mice per group for **a**: ND: 8, HFD: 8, HFD Live Akk Synthetic: 5, HFD Pasteurized Akk: 8, HFD Amuc_1100*: 9. Number of mice per group for **b** and **d**: ND: 8, HFD: 7, HFD Live Akk Synthetic: 8, HFD Pasteurized Akk: 10, HFD Amuc_1100*: 9. Number of mice per group for **c** and **e**: ND: 9, HFD: 7, HFD Live Akk Synthetic: 8, HFD Pasteurized Akk: 9, HFD Amuc_1100*: 9. Data were analyzed using one-way ANOVA followed by Tukey post-hoc test. * $P < 0.05$;** $P < 0.01$; *** $P < 0.001$.

Online Methods

Culture and pasteurization of *Akkermansia muciniphila*

A. muciniphila MucT (ATTC BAA-835) was cultured anaerobically in a basal mucin-based medium as previously described[9], or in a synthetic medium where mucin was replaced by 16 g/l soy-peptone, 4 g/l threonine, and a mix of glucose and N-acetylglucosamine (25 mM each). Cultures were washed and concentrated in anaerobic PBS with 25% (vol/vol) glycerol under strict anaerobic conditions. Additionally, an identical quantity of *A. muciniphila* grown on the synthetic medium was inactivated by pasteurization for 30 min at 70°C. Cultures were then immediately frozen and stored at -80 °C. A representative glycerol stock was thawed under anaerobic conditions to determine the CFU/ml by plate counting using mucin media containing 1% agarose (agar noble; Difco). Before administration by oral gavage, glycerol stocks were thawed under anaerobic conditions and diluted with anaerobic PBS to an end concentration of 2.10^8 CFU/150 µl and 2.5% glycerol.

Mice

Cohorts of 10 to 11-week-old male C57BL/6J mice (Charles River, L'Arbresle, France) were housed in a controlled environment (12h daylight cycle, lights off at 6 pm) in groups of two mice per cage, with free access to food and water. Upon delivery, mice underwent an acclimation period of one week, during which they were fed a control diet (ND) (AIN93Mi, Research Diet, New Brunswick, NJ, USA). At the beginning of each experiment, cages were randomly mixed to ensure that each group was matched in terms of body weight and fat mass. No blinding procedure was followed. Mice were fed a normal chow diet (ND) (AIN93Mi, Research diet, New Brunswick, NJ, USA) or a high-fat diet (HFD) (60% fat and 20% carbohydrates (kcal/100g) D12492i, Research diet, New Brunswick, NJ, USA). Body weight, food and water intake were recorded once weekly. Body composition was assessed by using 7.5MHz time domain-nuclear magnetic resonance (TD-NMR) (LF50 Minispec, Bruker, Rheinstetten, Germany). Mice experiments were not performed in a blinded manner.

For the first experiment, mice were treated daily with an oral administration of *A. muciniphila* grown on the mucus-based medium (HFD Akk M) or the synthetic medium (HFD Akk S). Additionally, one group of mice was treated daily with an oral administration of pasteurized *A. muciniphila* (HFD Akk P). Control groups (ND and HFD) were treated with an oral gavage of an equivalent volume of sterile PBS containing 2.5% glycerol. Treatment was continued for 4 weeks.

For the second experiment, mice were treated daily with an oral administration of either live or pasteurized *A. muciniphila* grown on the synthetic medium (HFD Akk S and HFD Akk P, respectively). Control groups (ND and HFD) were treated with an oral gavage of an equivalent volume of sterile PBS containing 2.5% glycerol. Treatment was continued for 5 weeks. Fresh urinary samples were collected during the final week of treatment and directly stored at -80°C before analysis. Circulating leptin and resistin concentrations were determined using a multiplex immunoassay kit (Merck Millipore, Brussels, Belgium) and measured using Luminex technology (Bioplex, Bio-Rad, Belgium) following the manufacturer's instructions. Circulating adiponectin concentrations were determined using an ELISA kit (R&D Systems, Minneapolis, Minnesota, USA). Fecal energy content was measured on fecal samples harvested after a 24h period during the final week of treatment by the use of a bomb calorimeter (Mouse Clinical Institute, Illkirch, France).

For the third experiment, mice were treated daily with an oral administration of either live or pasteurized *A. muciniphila* grown on the synthetic medium (HFD Akk S and HFD Akk P, respectively). Additionally, one group of mice was treated with a daily oral administration of 3 µg of the protein Amuc_1100* (see below) in an equivalent volume of sterile PBS containing 2.5% glycerol. This dose of Amuc_1100* was estimated to be equivalent to $1{,}5.10^8$ CFU of *A. muciniphila* through the use of an in-house polyclonal antibody. Control groups (ND and HFD) were treated with an oral gavage of an equivalent volume of of sterile PBS containing 2.5% glycerol. Treatment was continued for 5 weeks.

All mouse experiments were approved by and performed in accordance with the guidelines of the local ethics committee. Housing conditions were specified by the Belgian Law of May 29, 2013, regarding the protection of laboratory animals (agreement number LA1230314).

Exclusion criteria were predefined as follows: Mice displaying abnormal behavior under a HFD (e.g. increased aggressiveness leading to alteration of food intake and/or body weight loss) during the follow-up period were excluded from analyses. All tissues were carefully examined during necropsy and sampling. Any mouse displaying lesions (e.g. granulous liver) was also excluded. Finally, for all analyses and for each group, any exclusion decision was supported by the use of the Grubbs test for outlier detection. Moreover, during the second experiment, 2 mice from the same cage in the group HFD Akk S were excluded from analysis of the OGTT and insulin data displayed in figure S1d-g, because of aggressiveness and fighting throughout the OGTT leading to abnormal blood glucose and insulin values.

Oral glucose tolerance test

6h-fasted mice were treated with an oral gavage glucose load (2 g glucose per kg body weight). Blood glucose was measured before oral glucose load and 15, 30, 60, 90 and 120 min after oral glucose load. Blood glucose was determined with a glucose meter (Accu Check, Roche, Switzerland) on blood samples collected from the tip of the tail vein.

Insulin resistance index

Plasma insulin concentration was determined on samples using an ELISA kit (Mercodia, Uppsala, Sweden) according to the manufacturer's instructions. Insulin resistance index was determined by multiplying the area under the curve of both blood glucose (-30 to 120 min) and plasma insulin (-30 and 15 min) obtained following the oral glucose tolerance test.

Tissue sampling

At the end of the treatment period, animals were anesthetized with isoflurane (Forene®, Abbott, England) and blood was sampled from the portal and cava veins. After exsanguination, mice were killed by cervical dislocation. Subcutaneous adipose tissue depots, intestines and liver were precisely dissected, weighed and immediately immersed in liquid nitrogen and stored at -80°C for further analysis.

Histological analyses

Subcutaneous adipose tissue (SAT) depots and ileal tissue were fixed in 4% paraformaldehyde for 24 hours at room temperature. Samples were then immersed in ethanol 100% for 24 hours prior to processing for paraffin embedding. For the determination of Goblet cell density, ileal paraffin sections of 5 µm were stained with Periodic Acid Schiff (PAS) and counterstained with hematoxylin and eosin. Images were obtained using a SCN400 slide scanner and Digital Image Hub software (Leica Biosystems, Wetzlar, Germany). The number of goblet cells present on one

villus was quantified and divided by the villus length. A minimum of 5 villi were analyzed per mouse in a blinded manner.

For the SAT adipose tissue diameter, paraffin sections of 5 µm were stained with hematoxylin and eosin. Images were obtained using a SCN400 slide scanner and Digital Image Hub software (Leica Biosystems, Wetzlar, Germany). 5 high-magnification fields were selected at random for each mouse and adipocyte diameter was determined using ImageJ (Version 1.50a, National Institutes of Health, Bethesda, Maryland, USA).

Urinary metabonomics analyses

Mouse urine samples were prepared and measured on a spectrometer (Bruker) operating at 600.22 MHz 1H frequency according to previously published protocol[41]; the 1H NMR spectra were then processed and analyzed as described previously[18].

UPLC-MS/MS determination of plasma TMA and TMAO concentrations

Ultra-Performance Liquid Chromatography-Tandem Mass Spectrometry (UPLC-MS/MS) was employed for the determination of plasma TMA and TMAO. Plasma samples (10µL) were prepared as follows: I) samples were spiked with 10 µL Internal Standard (IS) solution ($^{13}C_3/^{15}N$-TMA, d_9-TMAO in water; 1 mg/l, Sigma-Aldrich). II) 45 µL of ethyl 2-bromoacetate solution (15g/l ethyl 2-bromoacetate, 1% NH4OH in acetonitrile) were added and derivatization of trimethylamines (TMA and $^{13}C_3/^{15}N$-TMA) to their ethoxy- analogues was completed after 30 minutes at room temperature. III) 935 µL of protein/lipid precipitation solution (94% acetonitrile/5%water/1% formic acid) was added; samples were centrifuged for 20 minutes (4°C, 20000g) and were transferred to UPLC-autosampler vials. Sample injections (5 µL loop) were performed to a Waters Acquity UPLC-Xevo TQ-S UPLC-MS/MS system equipped with an Acquity BEH HILIC (2.1×100 mm, 1.7 µm) chromatographic column. An isocratic elution was applied with 10 mM ammonium formate in 95:5 (v/v) acetronitrile:water for 7 minutes at 750µl/min and 50°C. Positive electrospray (ESI+) was used as ionisation source and mass spectrometer parameters were set as follows: capillary, cone and sources voltages at -700, -18 and 50 V respectively, desolvation temperature at 600°C, desolvation/cone/nebuliser gases were high purity nitrogen at 1000 l/hr, 150 l/hr and 7 bar respectively. Collision gas was high purity argon. Mass spectrometer was operated in multiple reaction monitoring (MRM) mode. The monitored transitions were the following: for derivatised-TMA, +146 → +118/59 m/z (23/27 V); for derivatised-$^{13}C_3/^{15}N$-TMA, +150 → +63/122 m/z (27/22V); for TMAO, +76 → +59/58 m/z (12/13 V); for d_9-TMAO, +85 → +68/66 m/z (18/20 V). The system was controlled by the MassLynx software, also used for the data acquisition and analysis.

RNA preparation and Real-time qPCR analysis

Total RNA was prepared from tissues using TriPure reagent (Roche). Quantification and integrity analysis of total RNA was performed by running 1 µl of each sample on an Agilent 2100 Bioanalyzer (Agilent RNA 6000 Nano Kit, Agilent). The cDNA was prepared by reverse transcription, and real-time qPCR was performed as previously described[8]. *RPL19* RNA was chosen as the housekeeping gene. Sequences of the primers used for real-time qPCR are available in Table S1.

Production of Amuc_1100* Protein

An expression plasmid for the production of His-tagged Amuc_1100, here termed Amuc_1100*, was constructed by amplification of its gene devoid of the coding sequence for its signal

sequence and cloning the resulting PCR product in pET-26b *E. coli* XL1Blue (Novagen®, Merck Millipore, MA, USA). The following primer sequences were used for the construct: 5'-GGGTAC**CATATG**ATCGTCAATTCCAAACGC-3' (Forward) and 5'-CCTTGG**CTCGAG**ATCTTCAGACGGTTCCTG-3' (Reverse). Bolded sequences are restriction sites for NdeI and XhoI enzymes, respectively (Thermoscientific, MA, USA).
Conformation of the resulting plasmid pET-26b-1100 was verified by sequence analysis and transformed into *E. coli* BL21 (DE3). This strain was then grown in LB-broth containing kanamycin (50 µg/ml) with shaking at 220 rpm at 37° C, followed by induction through the addition of 1mM IPTG in the growth medium during mid exponential phase. After three hours of induction, cells were pelleted by centrifuging 10 min at 5000 g and cell pellets stored at -20°C until lysis. Cell pellets were resuspended and lysed using lysozyme and sonification (Sonifier 450, Branson Ultrasonics Corporation, Danbury, CT, USA). Supernatant was collected after centrifugation and the Amuc_1100* protein purified by metal affinity purification under native conditions using Ni-16NTA His•Bind Resin (Novagen®, Merck Millipore, MA, USA). After buffer exchange using a Zeba spin column, the protein content was determined (BCA assay; Pierce, Rockford, IL, USA) and the Amuc_1100* protein was stored at -20°C.

Extraction of A. muciniphila LPS

A. muciniphila LPS was extracted using the hot phenol-water extraction method as described previously[42], with minor modifications. Briefly, bacterial cells from 5 ml overnight cultures were collected by centrifugation, washed once with water and resuspended into 500 µl of ultrapure water. The bacterial suspensions were warmed up at 65°C and then mixed with an equal volume of water-saturated phenol preheated to 65°C. The mixture was incubated at 65°C for 10 min and then transferred to ice to cool down. After centrifugation at 4°C for 5 min, the aqueous layer was carefully transferred to a new Eppendorf tube and the incubation with an equal volume of hot phenol was repeated twice. After this two volumes of acetone were added to the aqueous layer to precipitate LPS. The suspension was incubated at -20°C for two hours after which it was centrifuged at 4°C for 10 minutes and the pellet was dissolved in 50 µl of LPS-free water.

***In vitro* culture and stimulation of human HEK-Blue hTLR2/5/9/NOD2 cell lines.**

For the immune receptor stimulation analysis HEK-Blue hTLR2, hTLR5, hTLR9 and hNOD2 cell lines (Invivogen, CA, USA) were used. Cells were authenticated by Invivogen. Presence of mycoplasma contamination was assessed regularly through a PCR-based method. Stimulation of the receptors with the corresponding ligands activates NF-κB and AP-1, which induces the production of secreted embryonic alkaline phosphatase (SEAP), the levels of which were measured by spectrophotometer (Spectramax, Molecular Devices, CA, USA). All cell lines were grown and subcultured up to 70–80% of confluency using as a maintenance medium Dulbecco's Modified Eagle Medium (DMEM) supplemented with 4.5 g/l D-glucose, 50 U/ml penicillin, 50 µg/ml streptomycin, 100 µg/ml Normocin, 2 mM L-glutamine, and 10% (v/v) of heat-inactivated FBS. For each cell line, an immune response experiment was carried out by seeding HEK-blue cells in flat-bottom 96-well plates and stimulating them by addition of 20 µl bacterial suspensions. The 96-well plates were incubated for 20–24 h at 37°C in a 5% CO2 incubator. Receptor ligands Pam3CSK4 (10 ng/ml for hTLR2), RecFLA-ST (0.1 ng/ml for hTLR5), ODN 2006 (50 µM for hTLR9) and L18-MDP (0.1 ng/ml for hNOD2) were used as positive control whereas maintenance medium (DMEM) without any selective antibiotics was used as negative control. SEAP secretion was detected by measuring the OD600 at 1 h after addition of 180 µL of QUANTI-Blue (Invivogen) to 20 µL of induced HEK-Blue hTLR2/5/9/NOD2 supernatant.

Dynamic light scattering analysis

Heat induced aggregation of Amuc_1100* was measured by light scattering on a Carry Eclipse Fluoroscence spectrophotometer (Agilent Biosciences, Santa Clara, CA, USA) equipped with Cary temperature controller and thermophobes. Amuc_1100* (at the concentration of 15 µM) was heated in presence of PBS (pH 7.4) at a constant rate of 1°C /min from 30°C to 100°C. The light scattering at 350 nm was measured with excitation and emission slits at 2.5 nm.

Fast Protein Liquid Chromatography

Plasma total cholesterol and triglycerides (TG) were measured with commercial kits (CHOD-PAP for cholesterol and GPO-PAP for TG; BIOLABO SA, Maizy, France). Separation of plasma lipoproteins was performed using fast protein liquid chromatography (FPLC, AKTA purifier 10, GE Healthcare, Chicago, IL, USA). 50 µl of individual plasma was injected and lipoproteins were separated on Superose™ 6 10/300GL column (GE Healthcare, Chicago, IL, USA) with NaCl 0.15 M at pH 7.4 as mobile phase at a 1ml/min flow rate. The effluent was collected into fractions of 0.3 ml then cholesterol and TG content in each fraction were determined as described above. Quantification of cholesterol in lipoprotein classes (VLDL, LDL, and HDL) was performed by measuring the percentage peak area and by multiplying each percentage to the total amount of cholesterol.

Western-blot

To analyze the insulin signaling pathway in the third experiment, mice were allocated to either a saline-injected subgroup or an insulin-injected subgroup so that both subgroups were matched in terms of body weight and fat mass. They then received 1 mU insulin/g body weight (Actrapid; Novo Nordisk A/S, Denmark) under anesthesia with isoflurane (Forene®, Abbott, England), or an equal volume of saline solution into the portal vein. Three minutes after injection, mice were killed and liver was harvested.

For detection of proteins of the insulin signaling pathway, tissues were homogenized in ERK buffer (Triton X-100 0.1%, HEPES 50 mM, NaCl 5 M, Glycerol 10%, MgCl2 1.5mM and DTT 1mM) supplemented with a cocktail of protease inhibitors and phosphatase inhibitors. Equal amounts of proteins were separated by SDS–PAGE and transferred to nitrocellulose membranes. Membranes were incubated overnight at 4°C with antibodies diluted in Tris-buffered saline tween-20 containing 1% non-fat dry milk: p-IRβ (1:1,000; sc-25103, Santa Cruz, CA, USA), p-Akt^{Thr308} (1:1,000; #2965L, Cell Signaling, Danvers, MA, USA) and p-Akt^{Ser473} (1:1,000; #4060L, Cell Signaling). Quantification of phospho-proteins was performed on 5 animals with insulin injection and 5 animals with saline injection per group. The loading control was β-actin (1:10,000; ab6276).

Plasma LPS analysis

Portal vein plasma LPS concentration was measured using an Endosafe-Multi-Cartridge System (Charles River Laboratories, MA, USA), as previously described[8].

Safety assessment of live and pasteurized *A. muciniphila*

Results presented in this manuscript are *interim* safety reports from twenty subjects with excess body weight (Body mass index > 25 kg/m²) presenting a metabolic syndrome following the NCEP ATP III definition (any three of the five following criteria: fasting glycaemia > 110 mg/dl,

blood pressure ≥ 130/85 mm Hg or antihypertensive treatment, fasting triglyceridemia ≥ 150 mg/dl, HDL cholesterol < 40 mg/dl for males, 50 mg/dl for females, and/or waist circumference > 102 cm for males, 88 cm for females). Subjects were voluntarily recruited from the Cliniques Universitaires Saint-Luc, Brussels, Belgium between December 2015 and May 2016. Subjects were assigned to any of the treatment arms following a randomized block design. The exclusion criteria were: presence of acute or chronic progressive or chronic unstabilized diseases, alcohol consumption (> 2 glasses / day), previous bariatric surgery, any surgery in the 3 months prior to the study or planned in the next 6 months, pregnancy or pregnancy planned in the next 6 months, regular physical activity (> 30 min of sports 3 times a week), consumption of dietary supplements (omega-3 fatty acids, probiotics, prebiotics, plant stanols/sterols) in the month prior the study, inflammatory bowel disease or irritable bowel syndrome, diabetic gastrointestinal autonomic neuropathy (such as gastroparesis or reduced gastrointestinal motility), consumption of more than 30g of dietary fibers per day, consumption of vegetarian or unusual diet, lactose intolerance or milk protein allergy, gluten intolerance, current treatment with medications influencing parameters of interest (glucose-lowering drugs such as metformin, DPP-4 inhibitors, GLP-1 receptor agonists, acarbose, sulfonylueras, glinides, thiazolidinediones, SGLT2 inhibitors, insulin, lactulose, consumption of antibiotics in the 2 months prior the study, glucocorticoids, immunosuppressive agents, statins, fibrates, orlistat, cholestyramine, or ezetimibe), and baseline glycated hemoglobin (HbA1c) > 7.5%. The Commission d'Ethique Biomédicale Hospitalo-facultaire from the Université catholique de Louvain (Brussels, Belgium) provided ethical approval for this study and written informed consent was obtained from each participant. The trial was registered at clinicaltrials.gov as NCT02637115.

Subjects were assigned to receive either a daily dose of placebo (an equivalent volume of sterile PBS containing glycerol), 10^{10} CFU live *A. muciniphila* (Akk S - 10^{10}), 10^{9} CFU live *A. muciniphila* (Akk S – 10^{9}), or 10^{10} CFU pasteurized *A. muciniphila* (Akk P - 10^{10}) for 3 months (placebo and bacteria were produced at a food-grade level according to the HACCP quality system). Blood samples were collected at the beginning of the treatment and a portion was directly sent to the hospital laboratory to measure relevant clinical parameters. Different tubes were used based on the clinical parameter: EDTA-coated tubes for white blood cell count, Sodium fluoride-coated tubes for fasting glycemia, citrate-coated tubes for clotting assays, and lithium-heparin-coated tubes for urea and enzymatic activities. After 2 weeks of treatment, subjects came back to the hospital for a safety visit, where blood samples were collected to allow comparison of clinical parameters to baseline values. Both the subjects and the physicians were blinded to the treatment.

Statistical analysis

Mouse data are expressed as the mean ± SEM. Number of mice allocated per group was based on previous experiments investigating the effects of *Akkermansia muciniphila* on diet-induced obesity[8]. Variance was compared using a Bartlett's test. If variances were significantly different between groups, values were normalized by Log-transformation before proceeding to the analysis. Differences between groups were assessed using one-way ANOVA, followed by the Tukey post-hoc test. In cases when variance differed significantly between groups even after normalization, a Kruskal-Wallis test was performed, followed by the Dunnett post-hoc test. A two-way ANOVA analysis with a Bonferonni post-hoc test was performed for the evolution of glycemia and insulinemia during the OGTT, for the repartition of cholesterol and triglycerides in specific lipoproteins and for Western-blot analyses.

In vitro data are expressed as the mean ± SEM. Variance was compared using a Bartlett's test. If variances were significantly different between groups, values were normalized by Log-transformation before proceeding to the analysis. Differences between groups were assessed using one-way ANOVA, followed by a Dunns post-hoc test comparing all conditions to DMEM. In cases when variance differed significantly between groups even after normalization, a Kruskal-Wallis test was performed. For the dynamic light scattering analysis of Amuc_1100*, a Boltzmann – Sigmoid curve was fitted to the data.

Human data are expressed as the mean ± SD. Differences between groups were assessed using Kruskal-Wallis test. Differences between values observed at baseline and at the time of the safety visit were assessed using a Wilcoxon matched-pairs signed rank test. Data were analyzed using GraphPad Prism version 7.00 for Windows (GraphPad Software, San Diego, CA, USA).

Statistical comparisons were indicated with *,**,*** for $P < 0.05$, $P < 0.01$ and $P < 0.001$ respectively

Methods-only References

41. Dona, A.C.*, et al.* Precision high-throughput proton NMR spectroscopy of human urine, serum, and plasma for large-scale metabolic phenotyping. *Analytical chemistry* **86**, 9887-9894 (2014).
42. Zhang, L. & Skurnik, M. Isolation of an R- M+ mutant of Yersinia enterocolitica serotype O:8 and its application in construction of rough mutants utilizing mini-Tn5 derivatives and lipopolysaccharide-specific phage. *Journal of bacteriology* **176**, 1756-1760 (1994).

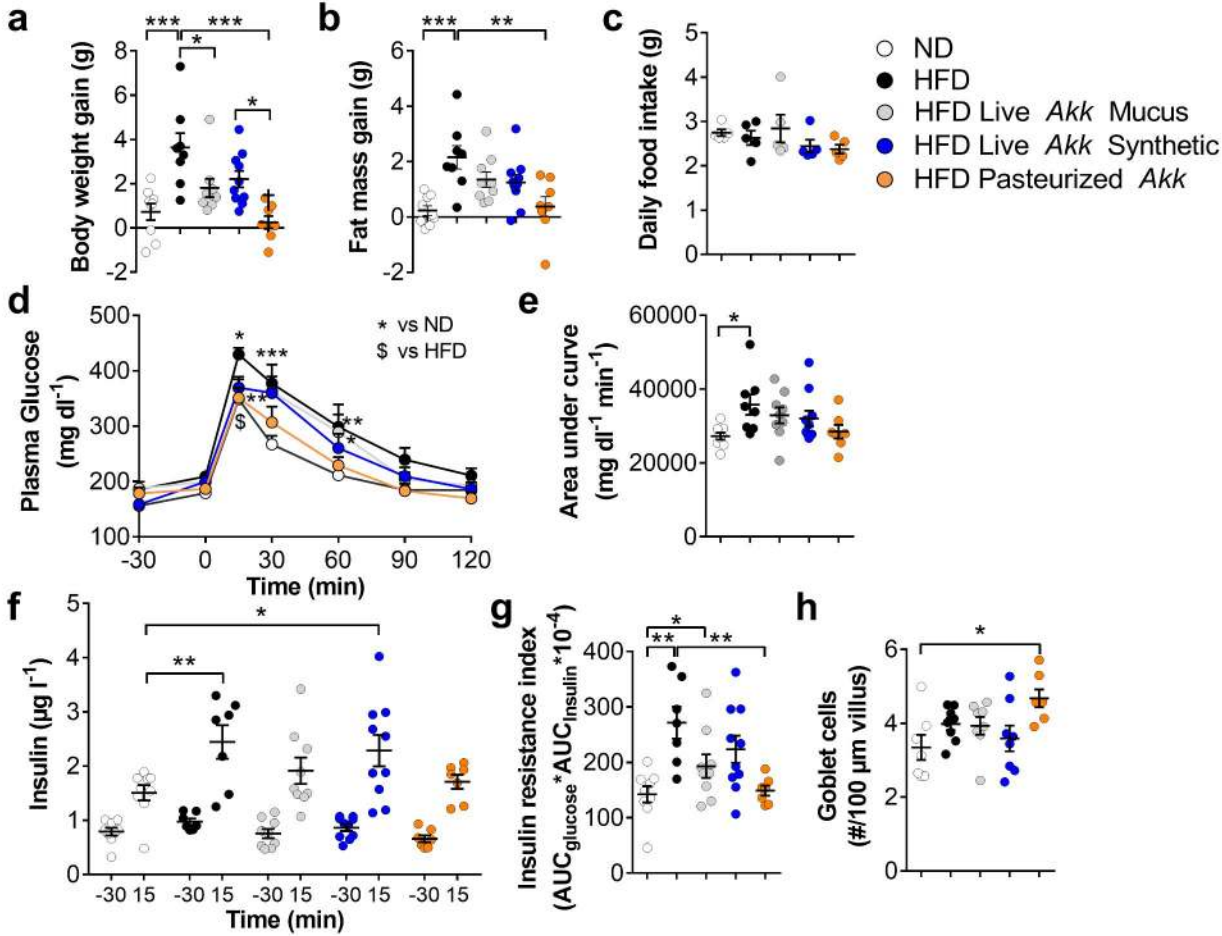
a
Body weight gain (g)
b
Fat mass gain (g)
c
Daily food intake (g)
ND
HFD
HFD Live Akk Mucus
HFD Live Akk Synthetic
HFD Pasteurized Akk
d
Plasma Glucose (mg dl-1)
* vs ND
$ vs HFD
Time (min)
e
Area under curve (mg dl-1 min-1)
f
Insulin (µg l-1)
Time (min)
g
Insulin resistance index (AUCglucose*AUCInsulin*10-4)
h
Goblet cells (#/100 µm villus)

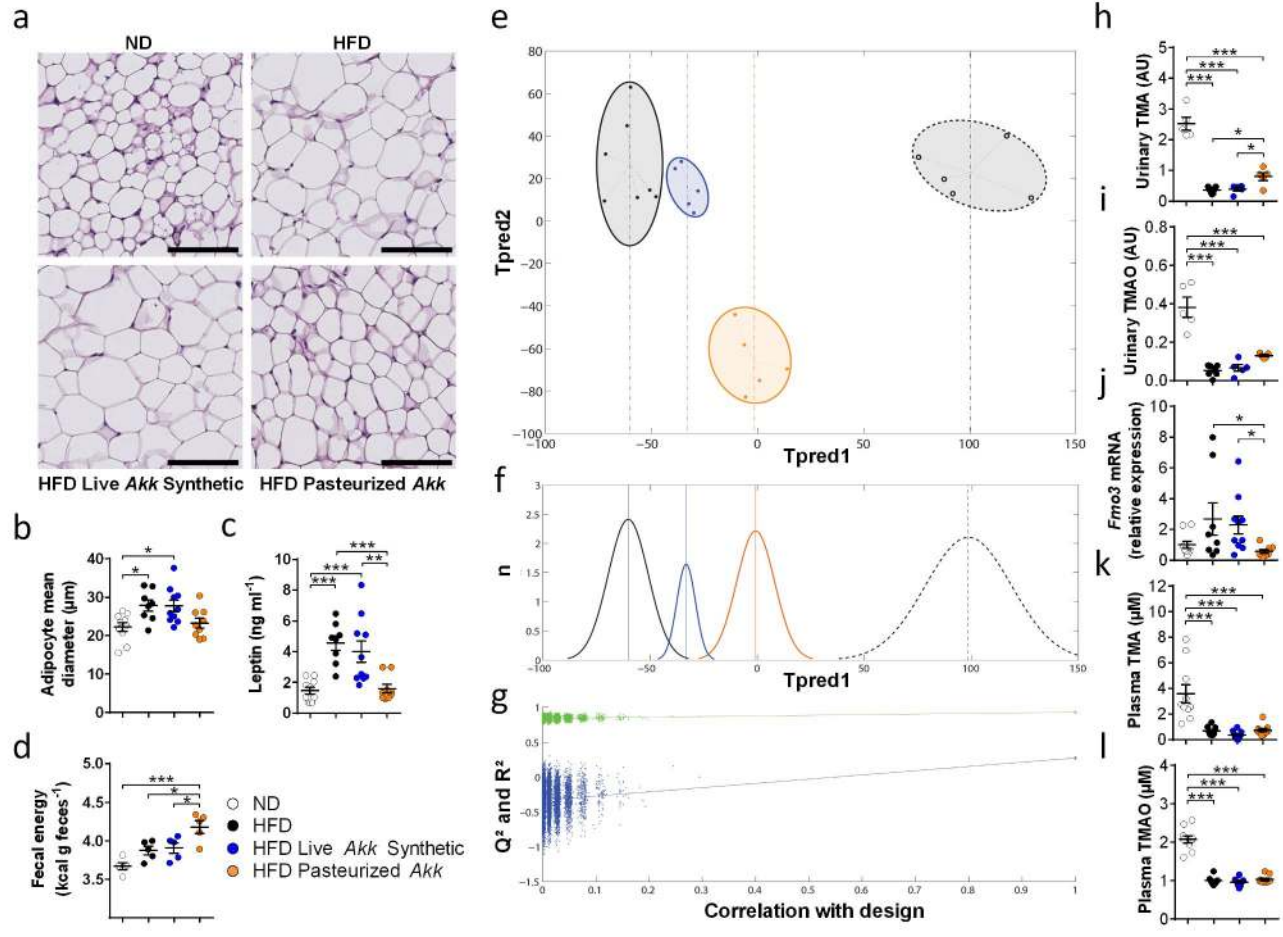
a
ND
HFD
HFD Live Akk Synthetic
HFD Pasteurized Akk
b
Adipocyte mean diameter (µm)
c
Leptin (ng ml-1)
d
Fecal energy (kcal g feces-1)
ND
HFD
HFD Live Akk Synthetic
HFD Pasteurized Akk
e
Tpred2
Tpred1
f
n
Tpred1
Q² and R²
Correlation with design
h
Urinary TMA (AU)
i
Urinary TMAO (AU)
j
Fmo3 mRNA (relative expression)
k
Plasma TMA (µM)
l
Plasma TMAO (µM)

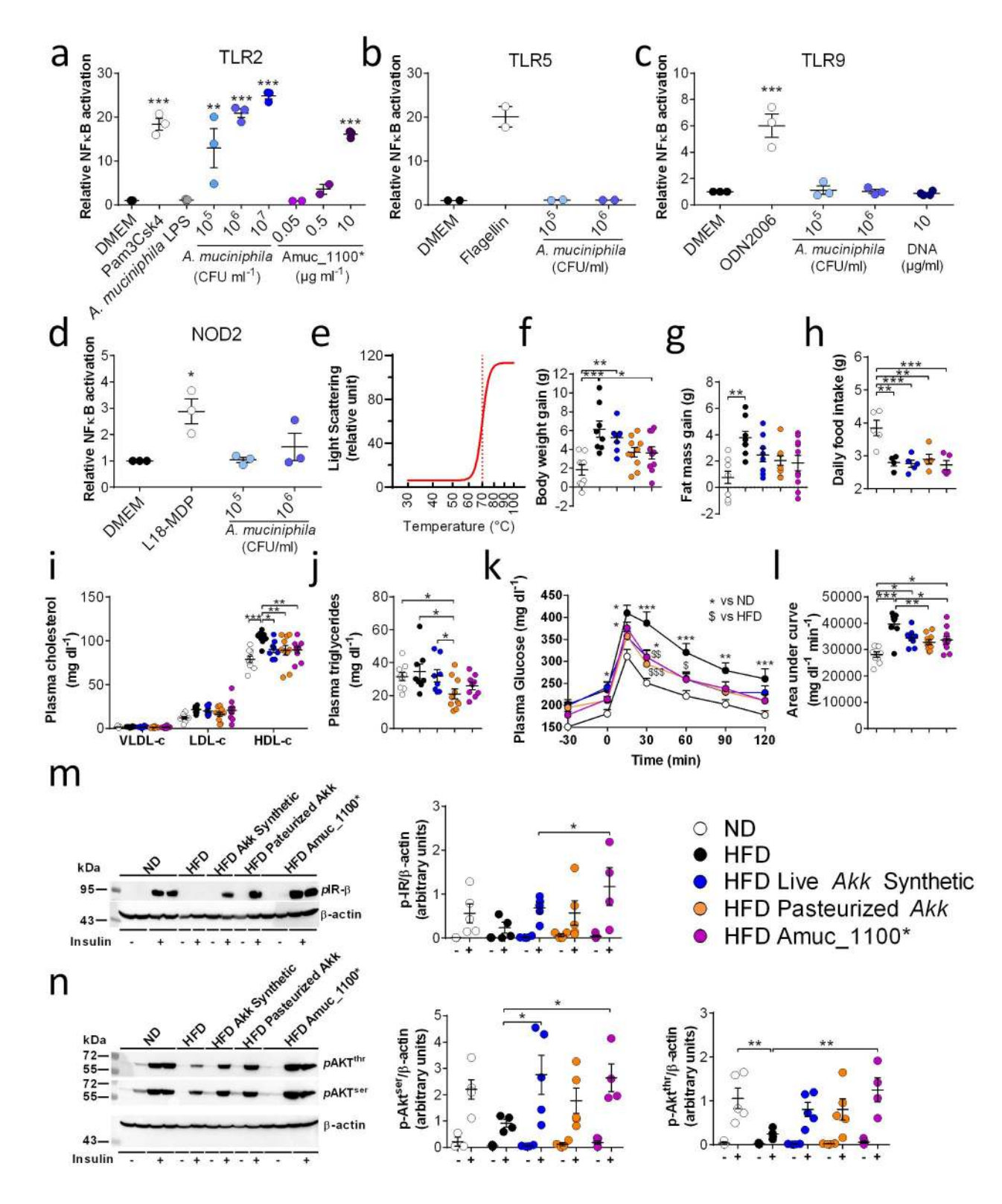
a
TLR2
Relative NFκB activation
DMEM
Pam3Csk4
A. muciniphila LPS
A. muciniphila (CFU ml-1)
Amuc_1100* (μg ml-1)
b
TLR5
DMEM
Flagellin
A. muciniphila (CFU/ml)
c
TLR9
DMEM
ODN2006
A. muciniphila (CFU/ml)
DNA (μg/ml)
d
NOD2
DMEM
L18-MDP
A. muciniphila (CFU/ml)
e
Light Scattering (relative unit)
Temperature (°C)
f
Body weight gain (g)
g
Fat mass gain (g)
h
Daily food intake (g)
i
Plasma cholesterol (mg dl-1)
VLDL-c
LDL-c
HDL-c
j
Plasma triglycerides (mg dl-1)
k
Plasma Glucose (mg dl-1)
* vs ND
$ vs HFD
Time (min)
l
Area under curve (mg dl-1 min-1)
m
kDa
ND
HFD
HFD Akk Synthetic
HFD Pasteurized Akk
HFD Amuc_1100*
95
43
pIR-β
β-actin
Insulin
p-IR/β-actin (arbitrary units)
n
72
55
pAKTthr
pAKTser
p-Aktser/β-actin (arbitrary units)
p-Aktthr/β-actin (arbitrary units)
ND
HFD
HFD Live Akk Synthetic
HFD Pasteurized Akk
HFD Amuc_1100*

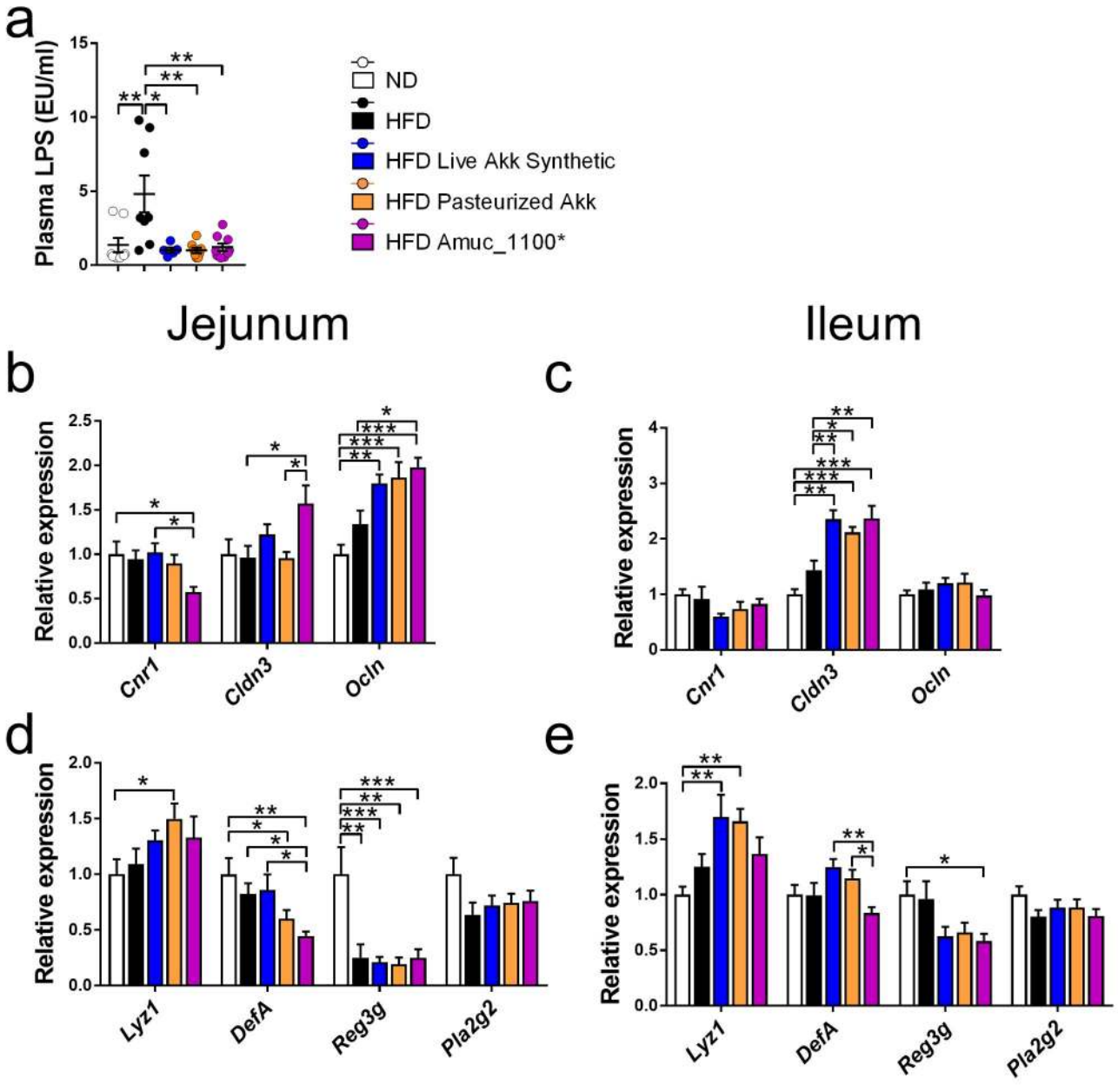
a
Plasma LPS (EU/ml)
ND
HFD
HFD Live Akk Synthetic
HFD Pasteurized Akk
HFD Amuc_1100*
Jejunum
Ileum
b
c
d
e
Relative expression
Cnr1
Cldn3
Ocln
Lyz1
DefA
Reg3g
Pla2g2